Supplement of Clim. Past, 10, 1967–1981, 2014
http://www.clim-past.net/10/1967/2014/
doi:10.5194/cp-10-1967-2014-supplement

Climate of the Past
Open Access

Supplement of

Hydroclimate variability of the northwestern Amazon Basin near the Andean foothills of Peru related to the South American Monsoon System during the last 1600 years

J. Apaéstegui et al.

Correspondence to: J. Apaéstegui (japaestegui@gmail.com)

Supplementary Information:

Analytical Methods

Age determinations were carried out at the Minnesota Isotope Laboratory (USA), using a multi-collector inductively coupled plasma mass spectrometry technique (MC-ICP-MS, Thermo-Finnigan NEPTUNE), according to the procedures described in Cheng et al., (2013). Twenty samples weighing between 150 and 300 mg were dissolved and equilibrated with a ^{236}U-^{233}U-^{229}Th spike and then separated and purified using methods described in Edwards et al. (1987). Initial ^{230}Th values were corrected with a typical bulk earth ratio, i.e. atomic ratio of ^{230}Th/^{232}Th = 4.4 ± 2.2 ppm. U-Th isotopic data and ages are shown in Supplemental Table S1.

Oxygen isotope ratios are expressed in δ notation, the per mil deviation from the VPDB standard. For example for oxygen, $\delta^{18}O = [((^{18}O/^{16}O)\ \text{sample}/\ (^{18}O/^{16}O)\text{VPDB}) - 1] \times 1000$. For each measurement in the PAL4 speleothem, approximately 200 μg of powder was drilled from the sample and analyzed with an on-line, automated, carbonate preparation system linked to a Finnigan Delta Plus Advantage. The speleothem reproducibility of standard materials is 0.1‰ for $\delta^{18}O$. For each measurement in the PAL3 speleothem, ≤20 μg of powder was drilled and analyzed using a Kiel IV carbonate device coupled to a MAT 253 mass spectrometer (Thermo Finningan) allowing analytical precision around ± 0.04 ‰ for $\delta^{13}C$ e ± 0.08 ‰ for $\delta^{18}O$. Both samples were analyzed in the *Laboratório de estudos Geodinamicos e Ambientais* at the University of Brasilia (UnB).

Figure S1:

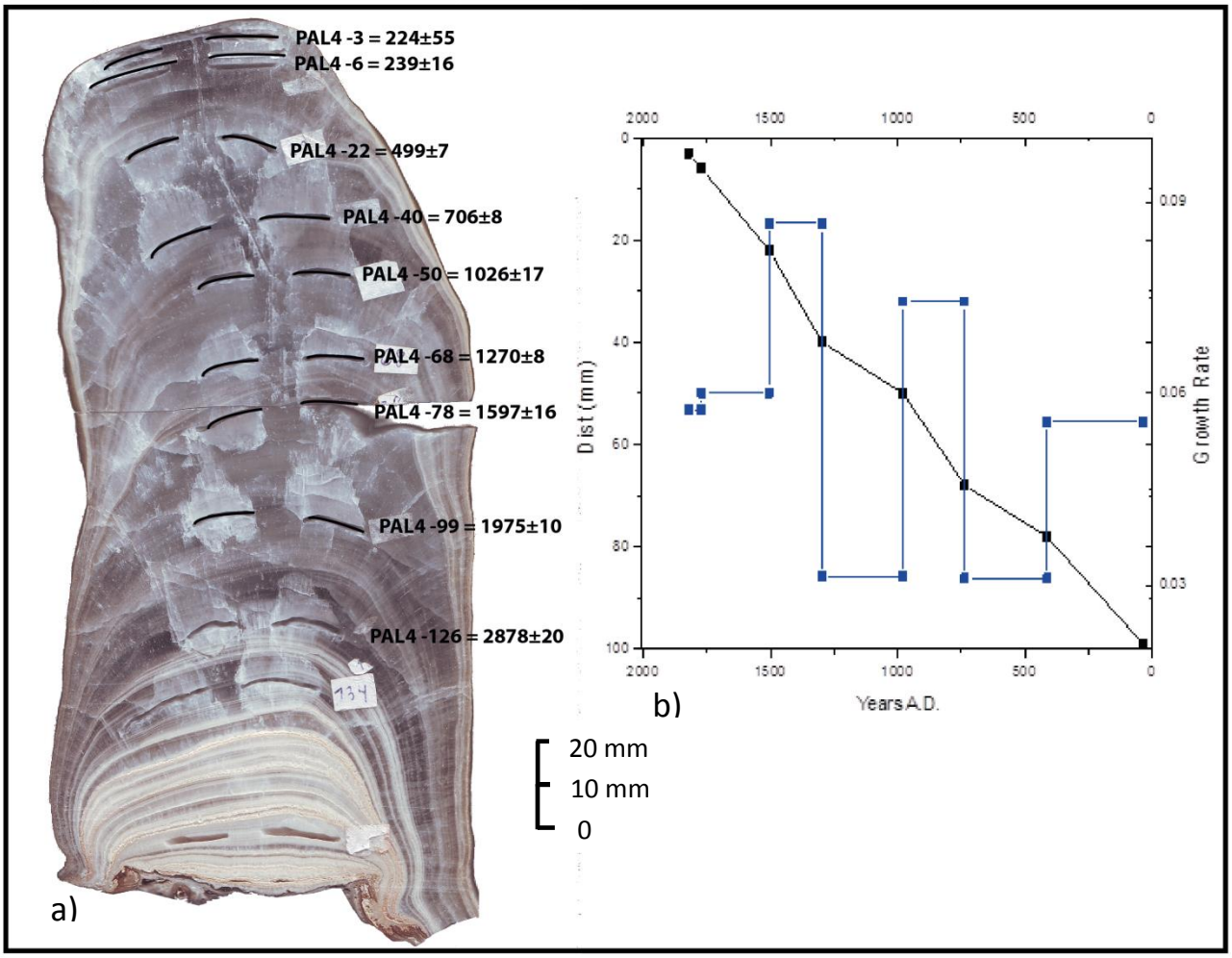

Figure S1: a) Pal4 speleothem and respective location of U-Th dates along the sample. b) Growth rate (blue line) and chronological model developed for the sample based on linear interpolation between dates (black line).

Figure S2:

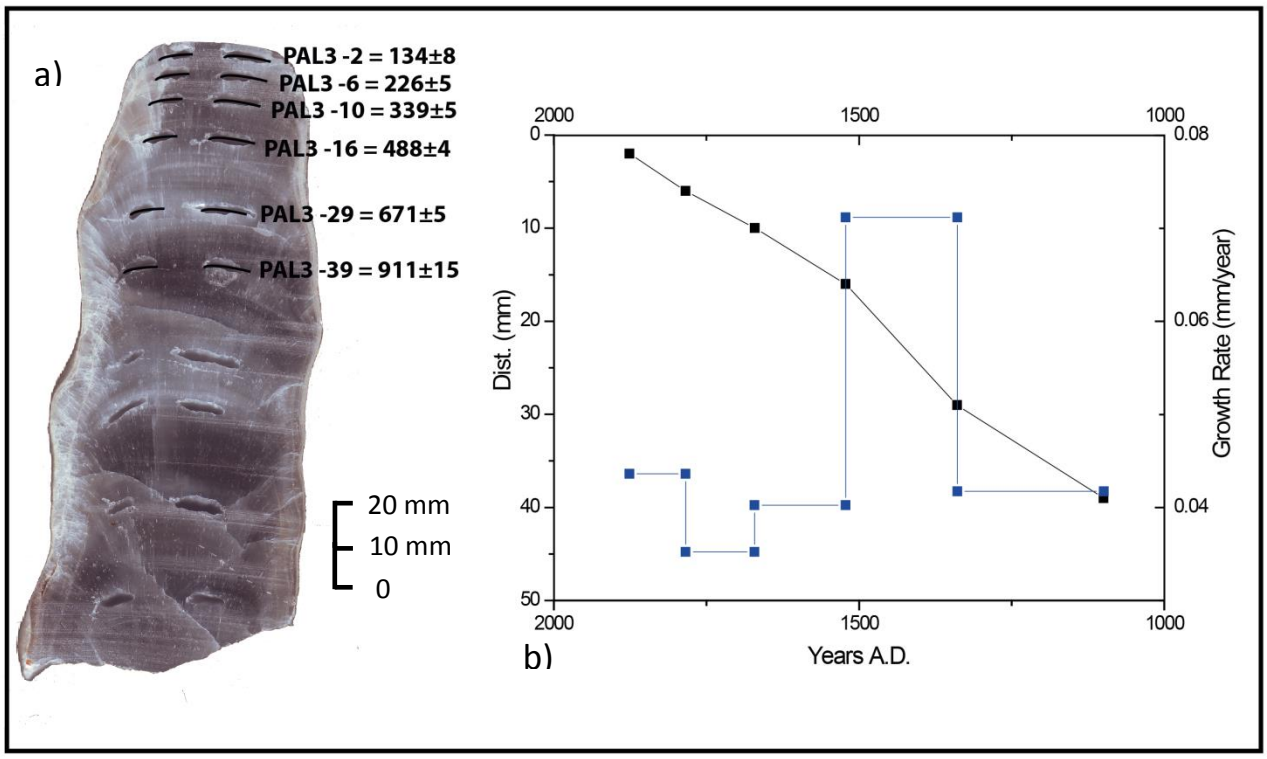

Figure S2: a) Pal3 speleothem and respective location of U-Th dates along the sample. b) Growth rate (blue line) and chronological model developed for the sample based on linear interpolation between dates (black line).

Figure S3

GMWL and LMWL

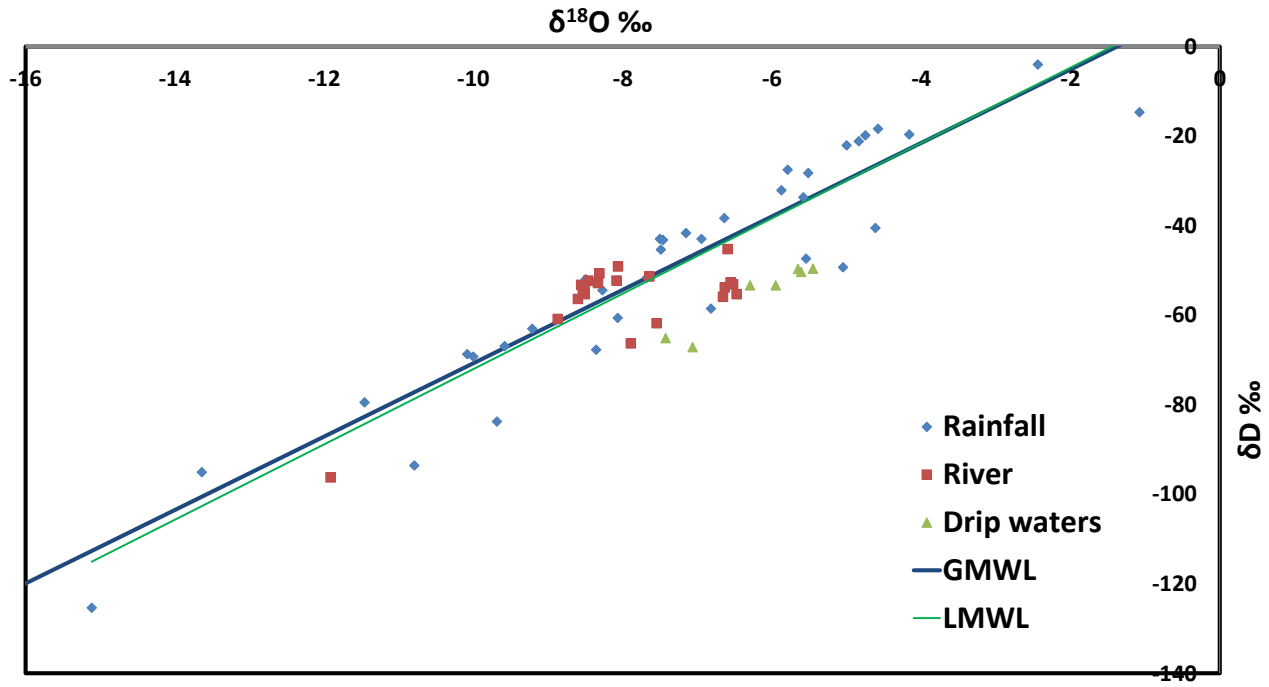

Figure S3: Isotope deuterium and oxygen values for waters sampled during monitoring program. Global Meteorological Water Line (GMWL, plotted in blue) and Local Meteorological Water Line (LMWL, plotted in cyan) show strong correspondence, indicating that equilibrium fractionation processes govern precipitation in this region.

Figure S4

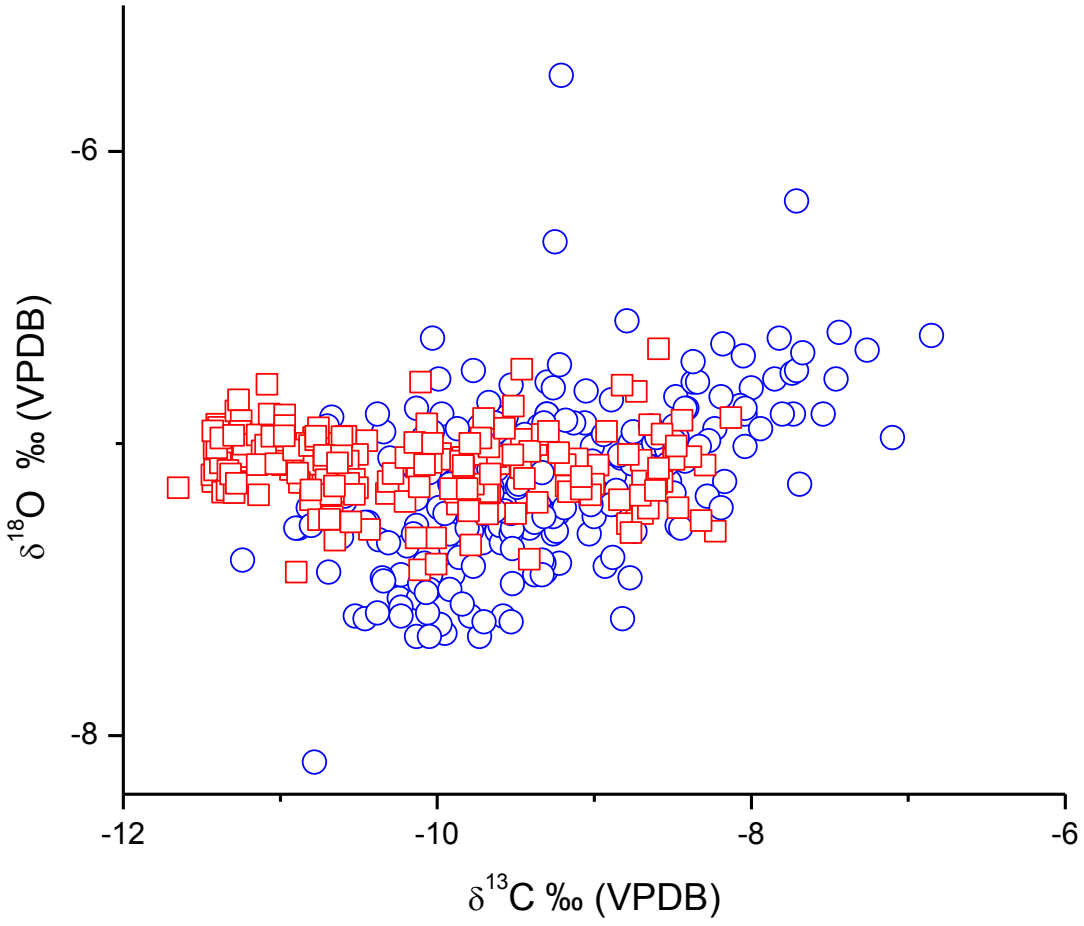

Figure S4: Scatter diagram of $\delta^{18}O$ versus $\delta^{13}C$ values for each analyzed stalagmite: blue circles indicate PAL4 stalagmite and red squares show PAL3 stalagmite.

Pal 4, R^2= 0.26 Pal 3, R^2 = 0.009

Figure S5

Spectral Analyses

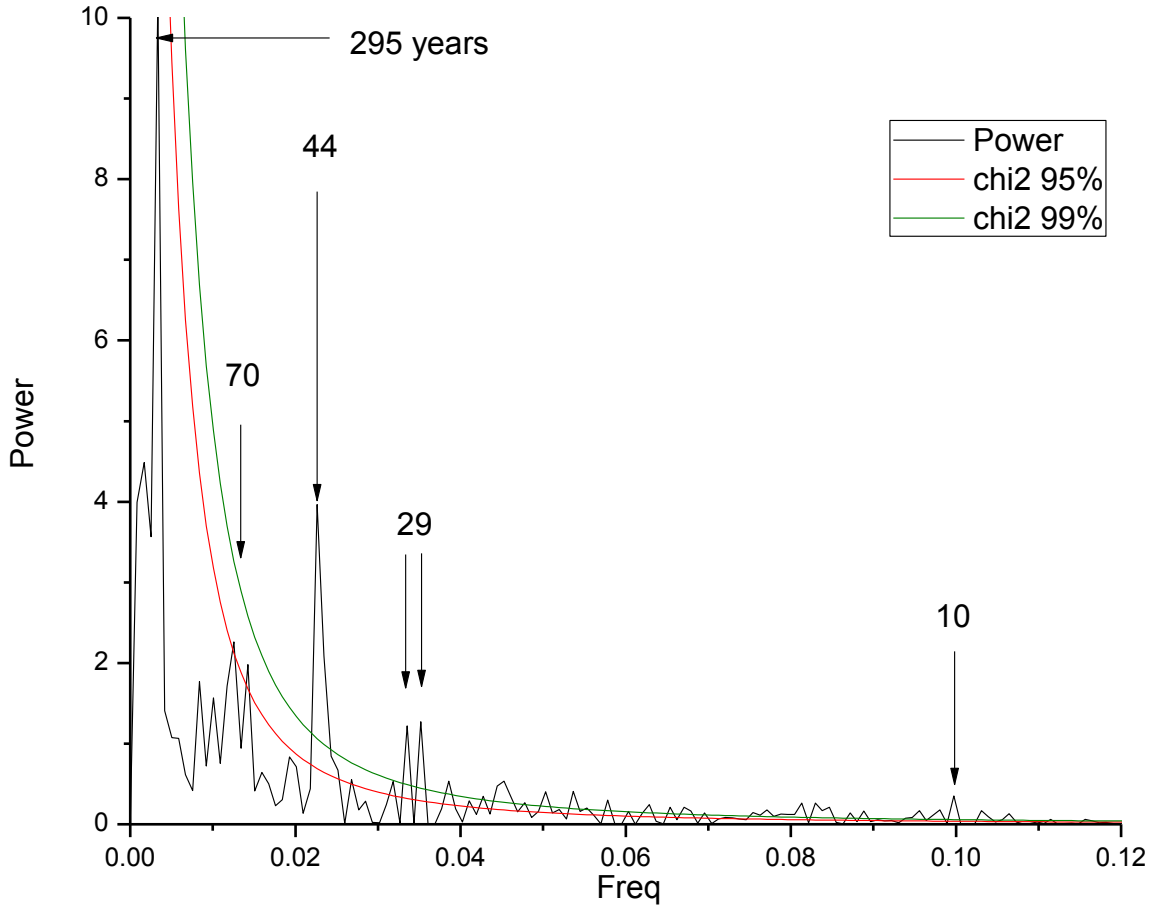

Figure S5: Spectral analysis of the $\delta^{18}O$ time series of Palestina record. Peaks that exceed the 90 % confidence level are labeled with their periods (in years). Analyses were performed with the Past software (Hammer et al., 2001) using the same routine of Schulz and Mudelsee, (2002), which uses the Lomb-Scargle periodogram for unevenly spaced data.

Figure S6

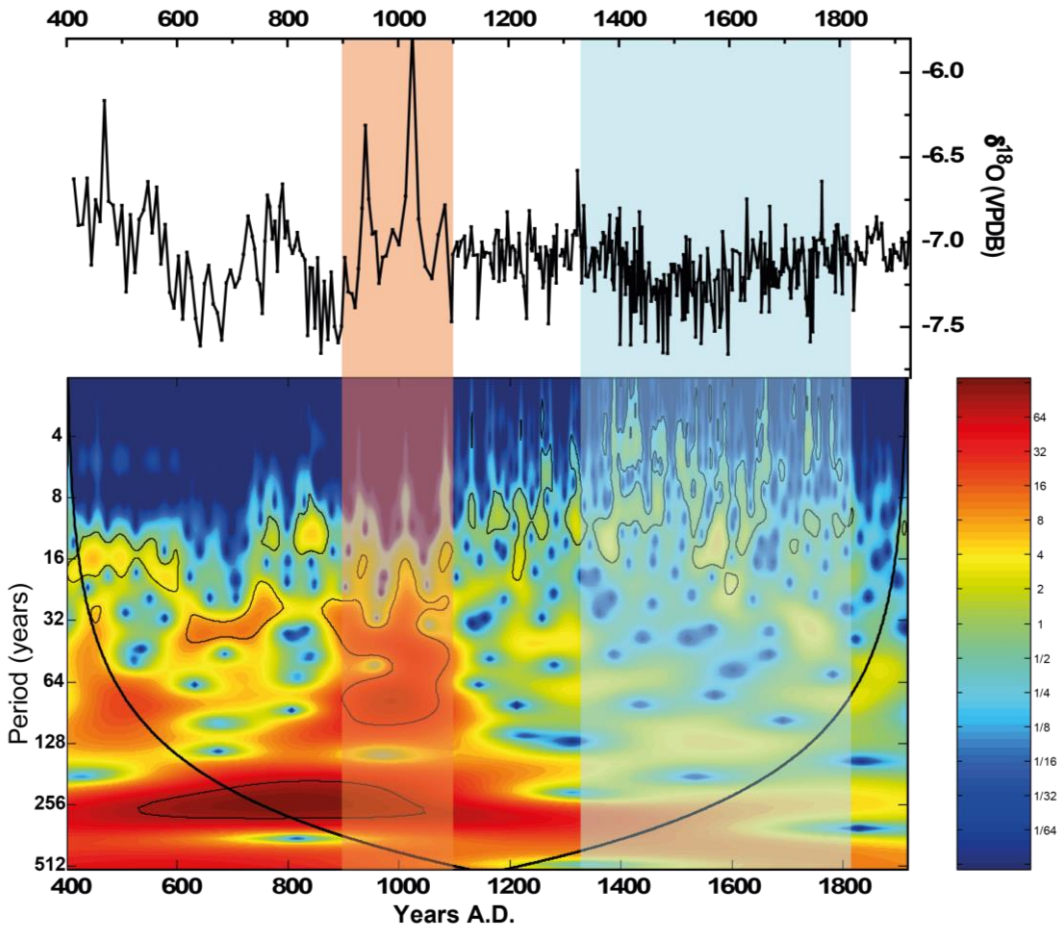

Figure S6: Time series and wavelet analysis of the Palestina record ($\delta^{18}O$). Red and light blue bars in the background represent the time period for MCA and LIA respectively.

Figure S7

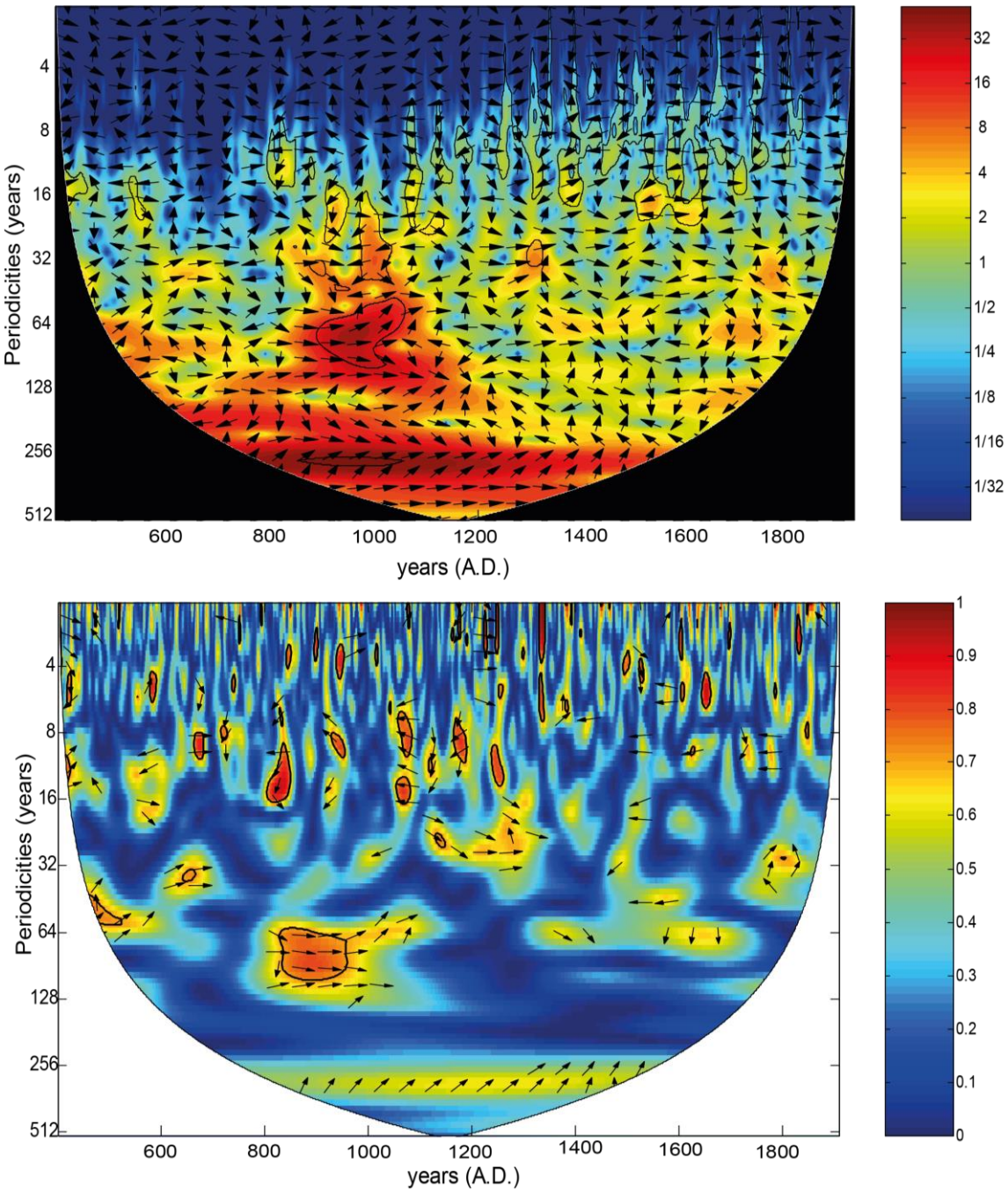

Figure S7: Cross-wavelets between Palestina and Pumacocha records (top) and coherence analysis (bottom) between time series.

Table S1

^{230}Th dating results. The error is 2σ error.

Sample Number	^{238}U (ppb)		^{232}Th (ppt)		^{230}Th / ^{232}Th (atomic x10^{-6})		δ^{234}U* (measured)		^{230}Th / ^{238}U (activity)		^{230}Th Age (yr) (uncorrected)		^{230}Th Age (yr) (corrected)	
PAL4-3	181	±0.4	1575	±32	17	±1	2271	±4	0.0090	±0.0002	301	±7	**224**	**±055**
PAL4-6	93.9	±0.1	131	±3	89	±5	2283.3	±3.1	0.0075	±0.0004	251	±14	**239**	**±16**
PAL4-11	230.0	±0.7	293	±6	122.2	±8.9	2306.2	±7.9	0.00943908	±0.00066	312	±22	**300**	**±23**
PAL4-16	422.5	±0.7	307	±7	285.6	±11.3	2289.2	±4.2	0.012608153	±0.00042	419	±14	**412**	**±15**
PAL4-22	349	±1.1	316	±6	279	±6	2293	±6	0.0153	±0.0001	507	±4	**499**	**±007**
PAL4-26	335.0	±0.9	231	±5	408.3	±13.1	2296.9	±6.6	0.017067833	±0.00041	566	±14	**560**	**±14**
PAL4-33	281.0	±0.9	144	±4	599.5	±25.8	2284.7	±7.8	0.018617254	±0.00064	619	±21	**615**	**±21**
PAL4-40	309	±0.5	288	±6	381	±8	2301	±5	0.0216	±0.0001	714	±5	**706**	**±008**
PAL4-46	220.9	±0.6	88	±3	1051.8	±40.7	2298.7	±6.9	0.025492211	±0.00063	845	±21	**842**	**±21**
PAL4-50	277	±0.4	692	±14	208	±4	2296	±4	0.0316	±0.0002	1048	±8	**1,026**	**±017**
PAL4-57	325.0	±1.0	278	±6	675	±18	2297.2	±8.1	0.035023	±0.0006	1163	±19	**1156**	**±20**
PAL4-68	360	±0.5	289	±6	790	±16	2294	±5	0.0384	±0.0002	1277	±6	**1,270**	**±008**
PAL4-78	94.7	±0.2	223	±5	341	±7	2302.9	±7.4	0.0487	±0.0004	1617	±14	**1597**	**±20**

*$\delta^{234}U = ([^{234}U/^{238}U]_{activity} - 1)x1000$.

** $\delta^{234}U_{initial}$ was calculated based on ^{230}Th age (T), i.e., $\delta^{234}U_{initial} = \delta^{234}U_{measured} \times e^{\lambda_{234} \times T}$.

Corrected ^{230}Th ages assume the initial $^{230}Th/^{232}Th$ atomic ratio of 4.4 ±2.2 x10^{-6}. Those are the values for a material at secular equilibrium, with the bulk earth $^{232}Th/^{238}U$ value of 3.8. The errors are arbitrarily assumed to be 50%.

Table S2

^{230}Th dating results. The error is 2σ error.

Sample Number	^{238}U (ppb)		^{232}Th (ppt)		^{230}Th / ^{232}Th (atomic x10^{-6})		δ^{234}U* (measured)		^{230}Th / ^{238}U (activity)		^{230}Th Age (yr) (uncorrected)		^{230}Th Age (yr) (corrected)	
PAL3-2	474	±1.1	499	±10	67	±3	2269.5	±5.0	0.0043	±0.0001	143	±5	**134**	**±8**
PAL3-6	442.2	±1.1	185	±4	271	±8	2273.7	±5.2	0.0069	±0.0001	229	±5	**226**	**±5**
PAL3-10	471.2	±1.2	149	±4	532	±14	2265.7	±5.5	0.0102	±0.0001	342	±4	**339**	**±5**
PAL3-16	497.6	±1.3	126	±3	952	±24	2264.5	±5.0	0.0147	±0.0001	491	±4	**488**	**±4**
PAL3-29	488.4	±1.3	78	±2	2065	±59	2264.5	±5.2	0.0201	±0.0001	672	±5	**671**	**±5**
PAL3-39	122	±0.4	16	±1	3403	±203	2268.6	±5.4	0.0272	±0.0004	912	±15	**911**	**±15**

*$\delta^{234}U = ([^{234}U/^{238}U]_{activity} - 1)x1000$.

** $\delta^{234}U_{initial}$ was calculated based on ^{230}Th age (T), i.e., $\delta^{234}U_{initial} = \delta^{234}U_{measured} \times e^{\lambda_{234} \times T}$.

Corrected ^{230}Th ages assume the initial $^{230}Th/^{232}Th$ atomic ratio of 4.4 ±2.2 x10^{-6}. Those are the values for a material at secular equilibrium, with the bulk earth $^{232}Th/^{238}U$ value of 3.8. The errors are arbitrarily assumed to be 50%.

Statistical Methods

The time series composite of the Palestina record is composed of 412 isotopic values of $\delta^{18}O$. The Palestina record was constructed by averaging the $\delta^{18}O$ records obtained from independent $\delta^{18}O$ time series from PAL4 and PAL3 speleothems. The sample resolution of the joint time series ranges between 1 to 10 years, depending on the period considered. The average resolution for the record is ~4 years; the resolution is lower during the MCA and higher for the LIA period.

Average values for the MCA and LIA period were calculated by averaging all available data corresponding to the periods from 900 for 1100 A.D. and from 1326 to 1820 A.D. respectively. Average values for both key periods were divided by their respective standard deviation, calculated for the period between 1922 and 734 A.D., which is the common period covered by all Andean records. The difference between LIA and MCA was calculated for each proxy and plotted in relation to their altitudinal and latitudinal locations in the main manuscript (Fig 5). The higher values observed in the more northern records, when compared with seasonality index derived over the Amazon Basin (Espinoza et al., 2008), suggest that higher seasonality could represent an additional important mechanism aside from SASM intensity to explain the difference between MCA and LIA periods.

In order to quantify the AMO influence over the South American records, composite analysis was performed on the $\delta^{18}O$ records based on different AMO thresholds. $\delta^{18}O$ composites were created for each proxy, averaging over all time epriods when the AMO index fell below the 25 percentile (AMO-) or remained above the 75 percentile (AMO+) of the AMO time series. A Student's t-test was employed to evaluate whether the departures in the $\delta^{18}O$ are significant at $p<0.1$. The results are represented as regional maps for both AMO+ and AMO-.

References cited

Cheng, H., Edwards, R. L., Shen, C., Polyak, V. J., Asmerom, Y., Woodhead, J., Hellstrom,. Wang, Y., Kong, X., Spötl, C., Wang, X., Alexander C.J.: Improvements in ^{230}Th dating, ^{230}Th and ^{234}U half-life values , and U – Th isotopic measurements by multi-collector inductively coupled plasma mass spectrometry. Earth Planet. Sc. Lett., 371-372, 82–91. doi:10.1016/j.epsl.2013.04.006, 2013.

Edwards, R.L., Chen, J.H., and Wasserburg, G.J.: ^{238}U–^{234}U–^{230}Th–^{232}Th systematics and the precise measurement of time over the past 500,000 years: Earth Planet. Sc. Lett., 81, 175–192, 1987.

Hammer, Ø., Harper, D.A.T., Ryan, P.D., 2001, PAST: Paleontological Statistics Software Package for Education and Data Analysis: Palaeontologia Electronica v. 4, 9. http://palaeo-electronica.org/2001_1/past/issue1_01.htm.

Haug, G., Hughen, K., Sigman, D.M., Peterson, L.C., Röhl, U.: Southward migration of the Intertropical Convergence Zone through the Holocene, Science, 293, 1304-1308, 2001.

Shen, C-C., Edwards, R. L., Cheng, H., Dorale, J. A., Thomas, R. B., Moran, S. B., Weinstein, S. E., Edmonds H. N.: Uranium and thorium isotopic and concentration measurements by magnetic sector inductively coupled plasma mass spectrometry, Chem. Geol., 185, 165-178, 2002.

Shulz, M.; Mudelsse, M.: REDFIT: estimating red-noise spectra directly from unevenly spaced paleoclimatic time series: Computers & Geosciences, v. 28, p. 421–426, 2002.

Torrence, C., Compo, G.P.: A Practical Guide to Wavelet Analysis: B. Am. Meteorol. Soc., 79, 61-78, 1998.

Wang, Y., Cheng, H., Edwards, R.L., He, Y., Kong, X. An, Z., Wu, J., Kelly, M. J., Dykoski, C. A., Li, X.:The Holocene Asian Monsoon: Links to solar changes and North Atlantic climate, Science, 308, 854-857, doi: 10.1126/science.1106296, 2005.